**Full paper**

# Development of a folding arm on an articulated mobile robot for plant disaster prevention

Nobutaka Matsumoto[a], Motoyasu Tanaka[a*], Mizuki Nakajima[a], Masahiro Fujita[b], and Kenjiro Tadakuma[b]

[a]*Department of Mechanical Intelligent Systems Engineering, Graduate School of Information Science and Engineering, The University of Electro-Communication, 1-5-1 Chofugaoka, Chofu, Tokyo, Japan*;
[b]*Department of Applied Information Sciences, Graduate School of Information Sciences, Tohoku University, 6-6-01 Aramaki Aza Aoba, Aoba-ku, Sendai, Miyagi, Japan*;

In this work, we develop a folding arm on an articulated mobile robot to inspect an industrial plant. The design targets of the arm, its operations, measurement ability, and mobility, were set for the task of inspecting an industrial plant. To accomplish the targets, we designed the folding arm considering both accessibility to high locations and the mobility of the articulated mobile robot to which it is attached. The arm has links, joints, dummy wheels, and sensors and enables the robot to which it is attached to manipulate objects, e.g. rotating valves, opening a door, or inspecting by accessing high locations. In addition, changing the posture of the arm and touching the dummy wheel in the arm to the surrounding terrain can reduce any negative effect of the arm on the robot's mobility when it encounters narrow spaces, stairs, steps, and trenches. The arm is controlled as a six degrees-of-freedom manipulator without redundancy by an operator who directly sets two joint angles. The effectiveness of the developed arm was demonstrated not only through experiments in a laboratory but also in a field test at the Plant Disaster Prevention Challenge of the World Robot Summit 2018.

**Keywords:** Folding arm, articulated mobile robot, rotating valves, opening doors, mobility, world robot summit

## 1. Introduction

Articulated mobile robots have many links serially connected by joints and can move on rough terrain, pass through narrow spaces, and move along the inside or outside of piping. Thus, many articulated mobile robots have been developed for search and rescue operations [1–5], in-pipe inspections [6–13], and inspection tasks inside nuclear reactors [14, 15].

One of the applications of an articulated mobile robot is inspection and disaster response in industrial plants. There are many narrow passages, stairs, and other obstacles in industrial plants. Thus, a plant inspection robot needs to have high mobility to navigate them. In addition, the robot needs to measure the values of gauges, open doors, and operate objects such as rotating valves using an end-effector [16–18]. The gauges and valves in a plant are located not only near the ground but also at locations high above the floor because it is assumed that they will be measured and operated by humans. Therefore, a plant inspection robot needs to access, inspect, and operate gauges and valves designed for humans.

The articulated mobile robot KR-II[15] has been developed to use in nuclear reactor plants. The robot has prismatic joints that move in the vertical direction and can climb stairs and move

---

*Corresponding author. Email: mtanaka@uec.ac.jp

over rough terrain. The robot can access high locations and operate objects using its installed long arm, as in [19, 20], because the robot is narrow but can make itself tall. In contrast, the inspection robot also needs to reduce its height to enter spaces with low overhead, for instance, when it passes under pipes. An articulated mobile robot that has links serially connected by rotational joints, e.g. ACM-R4 series [21–23] and T$^2$ Snake-3 [24, 25], can enter such spaces because it can make its height small. The robot can climb over a high step by raising its head along the step and can semiautonomously climb stairs [24]. In addition, the robot has the ability to rotate valves thanks to the installation of an end-effector on the robot's head [25]. However, it is difficult for the robot to access locations high above the ground by itself because the length of the links of the robot are short and the output torque of the joints is limited. Our goal is to develop a robot arm that enables an articulated mobile robot with rotational joints to carry out the inspection and operation of objects at locations high above the ground.

Most of the arms for inspection and operation have been installed on crawler robots [26–32]. A crawler robot (such as OCTPUS [32]), can handle a long and large arm because it has a large payload. However, if an articulated mobile robot is given a long and large arm, it could lose some of its ability to enter narrow spaces. In addition, the installation of such arm makes the robot unable to lift up its head from the ground because such an arm is usually heavy. This makes it difficult for the robot to climb up steps and stairs.

Arms that are stored within the body of the robot or in limited spaces have been developed in [33–35]. However, they do not have enough degrees of freedom (DOF) to operate an object. In addition, if such arm is installed on the head or tail of articulate mobile robots, the weight of the arm makes the robot unable to lift up its head or tail because the weight of such an arm is concentrated in one place. This seriously degrades the mobility of the robot.

In the present study, we developed a folding arm on the articulated mobile robot for plant inspection. The design targets for plant inspection were set considering the competition field and tasks of the Plant Disaster Prevention Challenge at the World Robot Summit [36, 37], which took place in Tokyo, Japan, in October 2018. The arm has many long links, joints, and dummy wheels, and can manipulate objects, e.g. rotating valves and opening doors, at 1 m high using an end-effector. When the robot moves without using the end-effector, the posture of the arm is appropriately changed to consider the mobility of the robot. The effectiveness of the developed arm has been demonstrated not only through experiments in the laboratory but also in field tests in WRS2018.

## 2.   Problem Setting and Design Target

The articulated mobile robot to which the developed arm is attached is the T$^2$ Snake-4 [38], which is an improved version of the T$^2$ Snake-3 [24]. The base part of T$^2$ Snake-4 has the pitch joints, yaw joints, and active wheels, as shown in Fig. 1. The robot can move forward/backward using rotation of the active wheels while changing its posture using rotating joints. The robot can enter narrow spaces because of its thin body, can climb high steps using the length of its body, and can climb up/down stairs by appropriately controlling its joints [38].

The themes of the Plant Disaster Prevention Challenge of the World Robot Summit (WRS2018) are daily inspections and emergency responses in industrial plants. In this section, we present the design targets for the developed arm considering the performance that is required when the entire robot, including the arm, inspects industrial plants according to the field and missions of WRS2018.

### 2.1   *Operation ability*

It is necessary for the robot to operate valves and doors during a plant inspection. Table 1 shows the valves used in WRS2018 and whether it they are treated as an operation target in this paper.
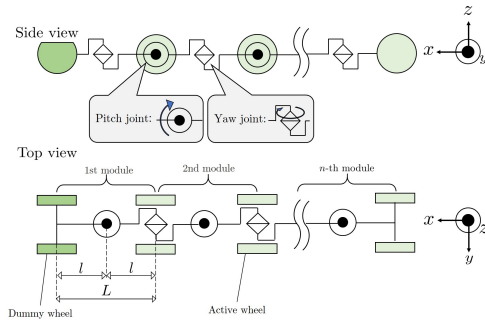
Figure 1. Model of the base part of the $T^2$ Snake-4.
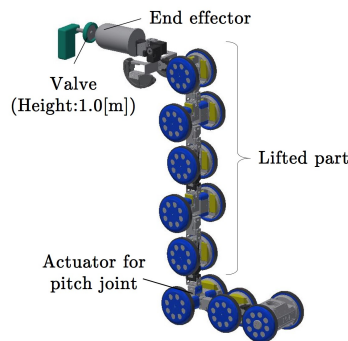


Figure 2. Posture of the $T^2$ Snake-4 without the arm approaching a valve at 1 m above the floor.

Table 1.   Valves in WRS2018 and the operation target

| Valve | Target / not |
| --- | --- |
| 15A ball valve | Target |
| 50A ball valve | Target |
| 80A ball valve | Target |
| 80A gate valve | - |
| 80A rubber seated gate valve | Target |

We did not consider the 80A gate valve as a design target because an end effector would become too large. The valves are located at various positions and orientations. The knob of a door is located at about 1 m above the floor, so the robot needs to lift up an end-effector to that height to operate doors. Thus, design target related to operations is the ability to operate valves and doors at a height of 1 m. $T^2$ Snake-3 was able to rotate a valve at a height of about 0.4 m in [25]. However, if the robot approaches a valve that is located high above the floor, it needs to lift many modules of the robot, as shown in Fig. 2, and the actuator of the pitch joint needs to generate large torque. In this case, the wheels and an excessive numbers of joints are lifted, even though these wheels are not used in the operation and the minimum number of joints needed to control the end effector is just six. If the pitch joint is designed considering such large torque, the size of the robot increases and its ability to enter narrow spaces degrades. In addition, the manufacturing cost increases because the number of modules of the robot must substantially increase in order to avoid falls. Therefore, we develop the arm considering both accessibility to high locations and the robot's ability to enter narrow spaces.

This aim of this study was to successfully complete the operations as a first step, so it does not consider inspection speed.

Table 2.   Target parameters related to mobility

|  | Value [mm] |
|---|---|
| Minimum width of the narrow path | 600 |
| Minimum height when sensors face upside | 660 |
| Minimum height when sensors face front | 1100 |
| Tread and riser of stair climbing | tread: 200, riser: 200 |

## 2.2   *Measurement ability*

The plant inspection robot needs sensors to inspect its surroundings, to measure gauges, and to detect faults in equipment. If the gauges are located assuming that a human will check them, they will be located at eye level. Therefore, we set two design targets related to information gathering. One is to install sensors on the robot for environment mapping and measuring gauges, surface temperature, concentration of carbon dioxide, and abnormal sounds based on missions of WRS2018. The other is to enable the robot to raise the sensor unit up to a height of 1.5 m (eye level).

## 2.3   *Effect on mobility*

The ability to enter narrow spaces is desirable for a plant inspection robot because passages in industrial plants are narrow. The ability to climb stairs is also needed in the case where an industrial plant has several floors. Assuming use in disaster response, the ability to climb over obstacles and cross trenches is also important.

If a long arm similar to the one on a crawler robot [26–32] is installed on the articulated mobile robot as, the ability of the robot to enter narrow spaces degrades because of the length of the long arm. If the arm does not touch the surroundings, the mobility of the robot degrades because its total weight increases and the actuator power of the robot is limited. In contrast, HELIOS IX[31] uses its arm for mobility, and is able to climb up a high step that it would not be able to without the arm. Thus, it is possible to improve the mobility of the robot by using the motion of the arm.

Therefore, our design target related to mobility is to enable the robot to enter narrow spaces and climb stairs in the field of WRS2018, as listed in Table 2. The minimum width was described in the rulebook of the competition, and the other targets were set using the CAD data of the competition field. There are two minimum heights, depending on where the sensors face, as shown in Fig. 3. Note that we did not consider mobility based on the field for the mission after a disaster because almost no prior information was provided. In addition, our non-binding design target related to mobility is to maintain or improve the robot's mobility with respect to the ability of the robot without the folding arm.

## 3.   Mechanical design

The design targets of the developed arm are summarized in Table 3. We selected the folding type arm that is composed of long links serially connected by joints. When the robot operates valves and doors using an end-effector, it can extensively approach objects using the DOF of the joints. When the robot locomotes, the arm changes its posture and a part of the arm contacts the surroundings to reduce the negative effect on the robot's mobility. In addition, we reduce the weight of the arm at the cost of its mechanical stiffness because an increase in weight significantly degrades the mobility of the robot. However, when the stiffness of the arm decreases, position error and vibration of the end-effector are apt to occur. The soft gripper Omni-Gripper [39] is used as an end-effector. It can grasp an object even when a slight position error occurs. This means that the gripper compensates for the disadvantages of an arm that has low stiffness.

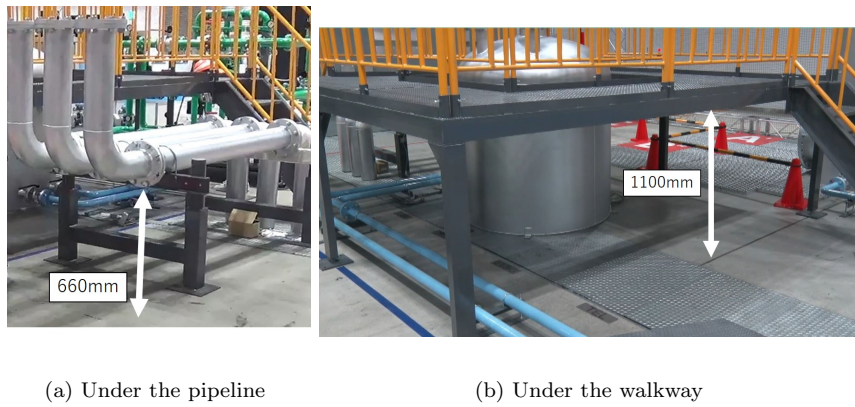(a) Under the pipeline                    (b) Under the walkway

Figure 3.   Two minimum heights. (a) The robot inspects the bottom surface of a pipeline from underneath it (sensors facing up), (b) the robot passes through without colliding with the upper walkway (sensors facing front).
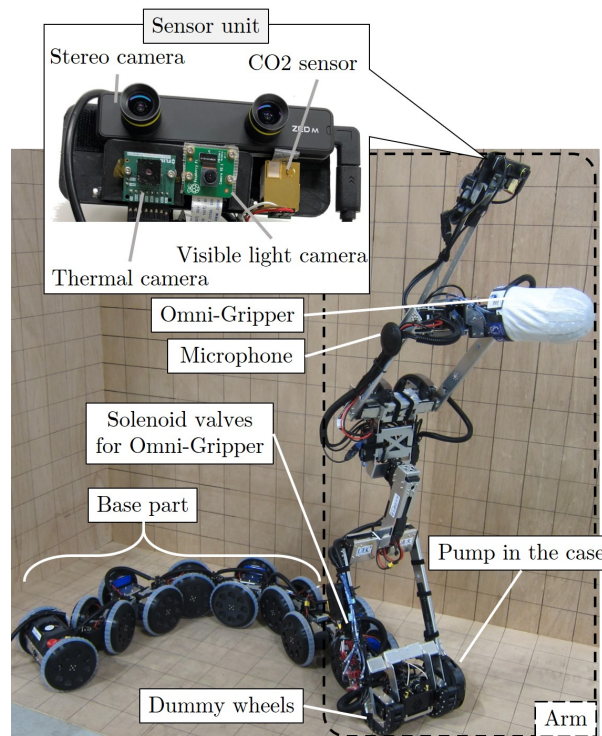


Figure 4. Developed folding arm attached to the $T^2$ Snake-4.

Figures 4 and 5 show the arm developed based on these concepts and its joint structure, respectively. Tables 4 and 5 show the parameters of the arm and the $T^2$ Snake-4, respectively. The arm has two pairs of dummy wheels that are located coaxially on the first and fourth joints, and the robot can locomote while letting the dummy wheels contact the surroundings. The rulebook of the Plant Disaster Prevention Challenge in WRS2018 notes that the field was "narrow in some sections: approx. 600 mm." Thus, we designed the folding arm to satisfy this limit (width < 600 mm) with a margin rather than meet the exact limit. The first–seventh joints are used to control the position and orientation of the end-effector, and the sensor joint is used to independently rotate the sensor unit. The rotational axes of the fifth, sixth, and seventh joints intersect at a point. Two actuators are used in parallel on the first, second, fourth, and fifth joints because these joints need to handle large loads. A mechanical stopper is attached on the first link to avoid the collision between the first and second pair of dummy wheels, as shown in

5

Table 3.   Summary of the design targets

| Property | |
| --- | --- |
| Operations | The end-effector can reach 1 m above the floor, and the arm can operate valves of Table 1 and doors. |
| Measurement ability | The arm has sensors that enable it to make an environment map and to measure gauges, surface temperature, carbon dioxide concentration, and abnormal sounds, and the sensor unit can reach 1.5 m above the floor. |
| Mobility | The robot can enter narrow spaces and climb stairs as Table 2. |
| Mobility (non-binding target) | Comparing with the ability of the robot without the folding arm, the robot's mobility (entering narrow spaces, climbing up a step, climbing stairs, or crossing a trench) is maintained or improved by the arm. |
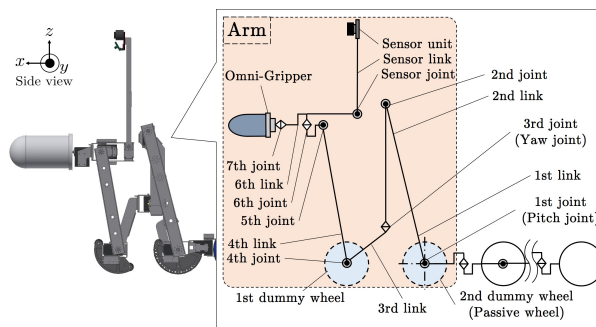


Figure 5.   Joint structure of the developed arm.

Table 4.   Parameters of the arm

| Parameters | Value |
| --- | --- |
| 1st link length [mm] | 370 |
| 2nd link length [mm] | 220 |
| 3rd link length [mm] | 166 |
| 4th link length [mm] | 300 |
| Sensor link length [mm] | 320 |
| Dummy wheel radius [mm] | 75 |
| Width of arm [mm] | 320 |
| Number of joints | 8 |
| Mass [kg] | 7.4 |

Fig. 6. The actuator Dynamixel XM540-W270 (Robotis Co., Ltd.) is used on the first, second, third, and fourth joints, and the actuator Dynamixel XM430-W350 (Robotis Co., Ltd.) is used on the other joints. A smart actuator unit such as the Dynamixel series has a microcontroller and sensors in the unit, and the joint angle and joint angular velocity can be controlled easily. In addition, the Dynamixel has a function that prevents breakage from overloading and overheating because it has sensors measuring the current and temperature. We selected the Dynamixel as the actuator because it can control the angle and angular velocity of the joint easily and it can improve the reliability of the entire system because of the function preventing breakage. The link structures are made from aluminium alloy 5052.
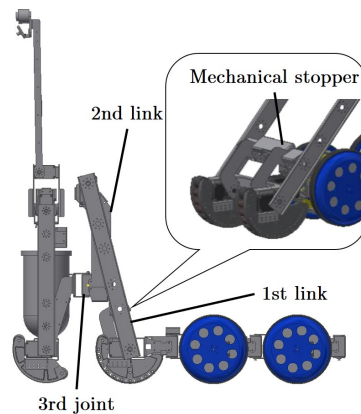
Figure 6. Mechanical stopper on the first link.

Table 5.   Parameters of T$^2$ Snake-4 with the arm

| Parameters | Value |
|---|---|
| Number of modules | 8 |
| Link length [mm] | 90.5 |
| Module length [mm] | 181 |
| Height* [mm] | 218 |
| Width [mm] | 320 (Arm) |
|  | 250 (Base part) |
| Length** [mm] | 1,598 |
| Wheel radius [mm] | 75 |
| Total mass [kg] | 20 |
| Battery life [min] | about 60 |

\*     Height     when     the     robot     is     in     a posture     that     minimizes     its     height.

\*\*     Length     without     the     arm     when     the robot     adopts     a     straight     posture.

### 3.1   *Operation using a soft gripper*

The soft gripper *Omni-Gripper* is attached to the tip of the arm. This is the improved version of the previous gripper of [39] to be resistant to cutting. By modulating the negative air pressure of the layer filled with granular material, the gripper can rapidly change its rigidity from the soft flowing state to the rigid jammed state. To envelop an object, the arm pushes the gripper in a soft deformable state. It can firmly grasp an object by becoming a rigid state. To rotate a valve, the seventh joint is rotated after the gripper grasping. To control the state of the gripper, a motor for pump and solenoid valves to select vacuuming up, applying pressure, or opening to atmospheric air pressure are installed in the robot.

The arm can extensively adjust the position and orientation of the end-effector because it has sufficient DOFs. The arm changes its posture, as shown in Figs. 7(A) and (B), when it accesses a valve from the side direction and from above, respectively. If the longitudinal direction of the gripper is parallel to the $xy$ plane, the end-effector can reach 1.1 m above the floor using the arm, as shown in Fig. 7(A). In addition, the soft gripper should be able to grasp the valves listed Table 1 and a doorknob because the shape of the gripper freely fits the object. Therefore, the design targets related to operations should be met by the folding arm with the soft gripper.

### 3.2   *Measurement ability*

The arm can raise the sensor unit up to a height of 1510 mm by changing its posture, as shown in Fig. 8. The sensor unit consists of a visible light camera for use when the end-effector is used,
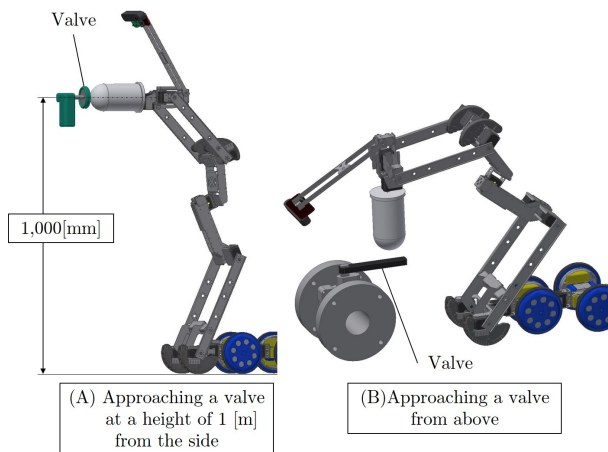
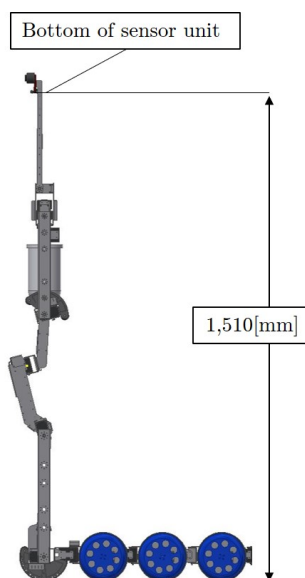Figure 7. The posture of the arm when operating valves.



Figure 8. Maximum height of the sensor unit.

a stereo vision camera for simultaneous visual localization and mapping, a thermal camera to detect abnormal temperature, and a $CO_2$ sensor to measure the concentration of carbon dioxide. In addition, the microphone is attached on the fourth link to detect abnormal noises. The robot gathers information using these sensors. Therefore, the design targets related to measurement ability have also been met.

### 3.3    Mobility

Figure 9 shows the posture of the arm when the robot locomotes without using the end-effector. The arm can be treated as one unit of the base part (a pair of wheels, yaw joint, and pitch joint) by appropriately changing its posture. We call the unit corresponding to the arm the *virtual module*.

   If the robot enters narrow passages or climbs stairs, the virtual module is used as shown in Fig. 9(A) and (B). The link lengths of the arm were designed considering the minimum height in Table 2 when the arm is used as a virtual module. When the arm is used as a virtual module and the sensor joint rotates as shown in Figs. 10(a) and (b), the maximum heights of the robot
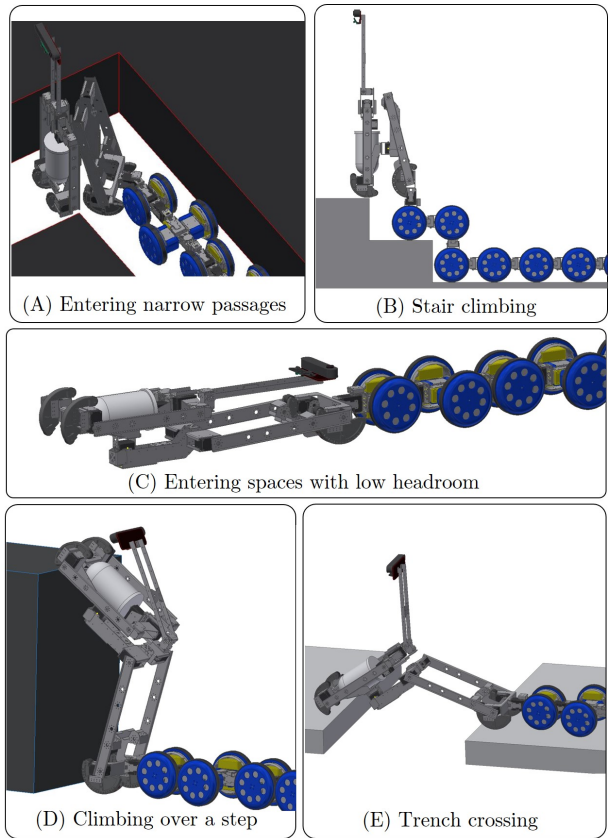
8

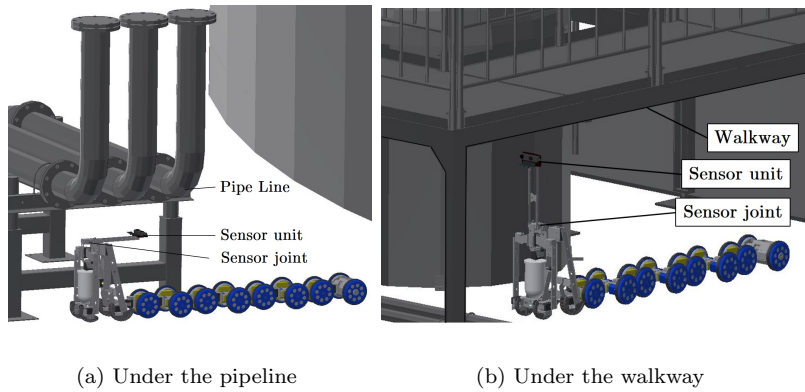Figure 9. Posture of the arm when the robot moves without using the end-effector.



Figure 10. The arm used as a virtual module when (a) the robot inspects the bottom surface of a pipeline from underneath it (sensors facing up) and (b) the robot passes through without colliding with the upper walkway (sensors facing front).

are 500 and 830 mm, respectively, and the design targets related to the minimum height in Table 2 are satisfied. The robot can enter a space with low headroom by changing the posture of the arm as shown in Fig. 9(C). In addition, the robot can climb over a step and cross a trench by changing the length of the virtual module as shown in Fig. 9(D) and (E).

Therefore, the design targets related to mobility should be met by introducing the virtual module and appropriately changing the posture of the arm.
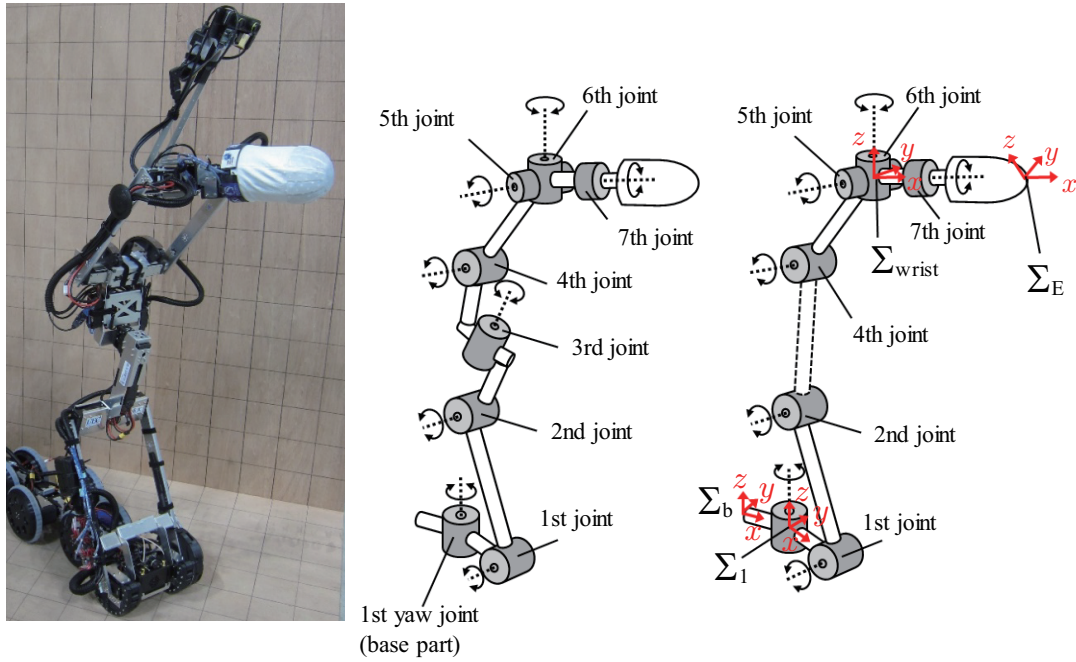
Figure 11.  Model of the arm for operation. The left panel shows the actual robot. The center and right panels depict an actual model of the arm and the control model, respectively.

## 4.    Controller

Three control modes are implemented in the robot: basic steering, stair climbing, and the control of the end-effector. The basic steering and stair climbing methods are described in [38]. This section describes the control method for an end-effector using the developed folding arm.

Figure 11 shows the model of the arm for operation using the end-effector. We use not only the joints of the arm but also the first yaw joint of the base part. This increases the operation area of the arm, similar to the operation of articulated robot arms. Let the basic coordinate system of the base part be $\Sigma_{\mathrm{b}}$, the coordinate system of the head link of the base part be $\Sigma_1$, the coordinate system of the tip of the end-effector be $\Sigma_{\mathrm{E}}$, and the wrist coordinate system whose origin is the intersection of the rotational axes of the fifth, sixth, and seventh joints be $\Sigma_{\mathrm{wrist}}$, as shown in the right figure of Fig. 11. Let unit vectors of the $x$, $y$, and $z$ axes in $\Sigma_{\mathrm{wrist}}$ be $\boldsymbol{e}_{xW}$, $\boldsymbol{e}_{yW}$, and $\boldsymbol{e}_{zW}$, respectively.

### 4.1    *Control of the end-effector*

The position and orientation of the end-effector are controlled to rotate valves and open doors. In this case, the arm has kinematic redundancy, because the number of joints that can be used to control the end-effector is eight. If kinematic redundancy is automatically used, it is difficult for the operator to understand the changes in the posture of the arm when the operator sends the command for the target motion of the end-effector. This increases the risk of falls and collision between the arm and the surroundings. Thus, the angles of two joints are fixed or directly controlled by the operator. As a result, the arm is controlled as 6-DOF manipulator without redundancy.

The commands of the operator are as follows.

- When not changing the orientation: the position of $\Sigma_{\mathrm{wrist}}$.
- When changing the orientation: the angles of the fifth, sixth, and seventh joints.
- The angle of the first joint of the arm.
- Forward/backward motion of the base part.

10

Table 6.   Results of valve operation tasks.

| Valve size | Located height[mm] | Result (Laboratory) | Result (WRS2018) |
|---|---|---|---|
| 15A ball valve | 1200 | Success | Success |
| 50A ball valve | 270 | Success | Success |
| 80A ball valve | 400 | Failure | No try |
| 80A gate valve | 650 | Unable | No try |
| 80A rubber seated gate valve | 875 | Success | Partial success* |

*The robot could rotate the valve but the rotation angle was not correct.

When the robot operates an object using the end-effector, it is difficult for the operator to understand $\Sigma_b$ because the operator sees only the view of the visible light camera on the sensor unit. It is also difficult for the operator to understand $\Sigma_E$ because the soft gripper is symmetric around the $x$ axis of $\Sigma_E$. In addition, error between a predefined $\Sigma_E$ and the actual position of the tip of the gripper occurs because the soft gripper changes its shape by contact with an object or by gravity. Thus, the target position is provided by the operator based on not $\Sigma_E$ but on $\Sigma_{wrist}$. The orientation of the end-effector is also provided by the operator based on $\Sigma_{wrist}$. From the geometric relationship, the rotation around $\boldsymbol{e}_{xW}$, $\boldsymbol{e}_{yW}$, and $\boldsymbol{e}_{zW}$ corresponds to the motion of the seventh, fifth, and sixth joints, respectively. Thus, the operator controls the orientation of the end-effector by directly changing the target angle of these joints.

To eliminate redundancy, the angle of the third joint is fixed to zero and the angle of the first joint is directly controlled by the operator. As a result, the DOF of the arm to control the end-effector is six without redundancy. The first joint gives the greatest effect when changing the center of mass of the arm and the height of the end-effector. The operator can intuitively change the posture of the arm and the position of the center of mass by directly changing the angle of the first joint. In addition, if the angle of the third joint is zero, the analytical solution of inverse kinematics is easily obtained because the direction of the rotational axes of the first, second, fourth, and fifth joints are equal. The analytical solution of the inverse kinematics is obtained in [41, 42].

### 4.2   *Control of the base part*

All joints and wheels on the base part except for the first yaw joint rest when the end-effector is controlled. However, when instructed by the operator, the base part can move forward/backward using the basic steering control [38]. The base part moves along the $x$ axis of $\Sigma_1$ while maintaining the position and orientation of the end-effector.

### 5.   Experiments

We carried out experiments not only in the laboratory but also in the field test of the Plant Disaster Prevention Challenge in the World Robot Summit 2018 (WRS2018) [40] to demonstrate the effectiveness of the developed folding arm. In this challenge, a competition was conducted in which the robots inspected and responded to disasters in a field imitating an industrial plant. This paper describes the results of operating valves using the arm in WRS2018, and another paper [38] describes the results of mobility and measurement abilities of the entire system of the $T^2$ Snake-4.

### 5.1   *Rotating valves*

The size and located height of the valves in the laboratory correspond to those in WRS2018. We set the target rotational angle to 90 deg. Table 6 shows the experimental results. The robot
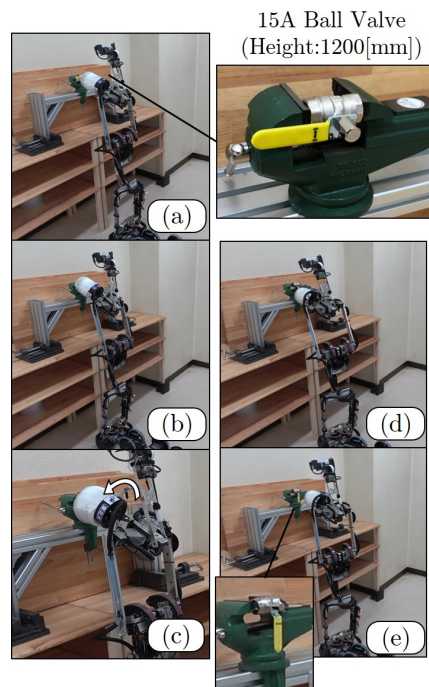
Figure 12.   Operating the 15A ball valve. (a) Approaching the valve, (b) grasping the valve, (c) and (d) rotating the valve, and (e) after letting go of the valve.

cannot rotate the 80A gate valve because the handle of the valve is so large that the gripper cannot envelop it.

If $\boldsymbol{e}_{xW}$ is parallel to the floor, the maximum height of the tip of the gripper is 1.1 m. However, the robot rotated the 15A ball valve at 1.2 m height in both the laboratory and at WRS2018, as Fig. 12 show. These results were possible thanks to the gripper's robustness against position error.

Figures 13 and 14 show the results of rotating the 50A ball valve. The valve is near the floor. The robot could rotate the valve when approaching it from above, as Fig. 13 shows, and from the side, as shown in Fig. 14. When approaching the valve from above, the arm was controlled by the method described in this paper. In contrast, when approaching from side, the robot adjusted the height of the gripper while letting the dummy wheels contact the ground, and the valve was rotated by letting the entire robot move forward using the basic steering method. The reason why such a method was used is that the ceiling was low in the place where the valve was installed and the robot could not lift up the arm high.

As Fig. 15 shows, the robot could not rotate the 80A ball valve because the grasp could not be maintained. The cause of failure is considered to be that the handle of the valve was too large for the gripper to appropriately envelop it, and the force of the robot pushing the gripper against the handle was not enough.

The robot could rotate the 80A rubber seated gate valve as Fig. 16 shows. At WRS2018, the target rotational angle was 180 deg. However, the robot could not appropriately rotate it, as Fig. 17 shows. The operator could not understand the situation because the orientation of the camera in the sensor unit was not appropriate and the operator could not see both the gripper and valve handle when the robot pushed the gripper against the valve. Therefore, the gripper could not appropriately grasp the valve, and slip between the gripper and valve occurred.

## 5.2   *Opening doors*

There was no door at WRS2018, but there are generally doors in a building for people to pass through. Thus, experiments opening doors have been carried out. The knob of the door is a
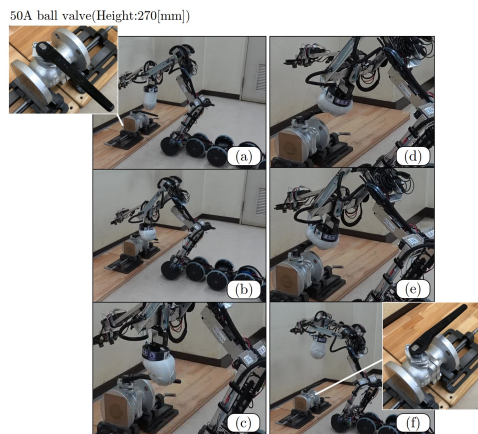
Figure 13.   Operating the 50A ball valve. (a) Approaching the valve, (b) and (c) grasping the valve, and (d) and (e) rotating the valve.
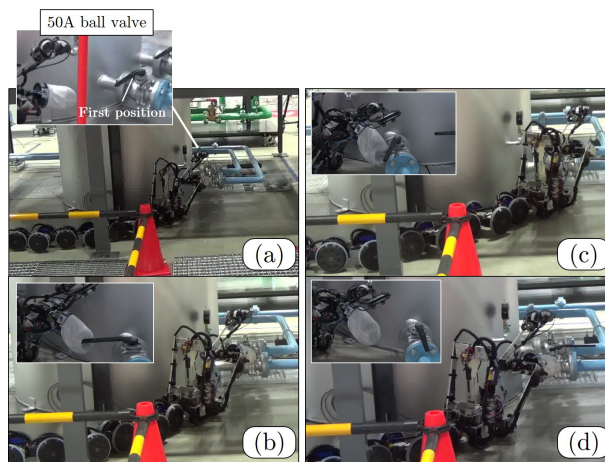


Figure 14.  Operating the 50A ball valve at WRS2018 [44].

lever handle. The door does not automatically close after the robot opens it because the door does not have spring-loaded hinges. Figures 18 and 19 shows the results of pushing and pulling the door. The robot approached the knob, grasped it using the gripper, rotated the knob, and pushed or pulled the door. Thus, the robot could open the door in both cases.

If the door has a spring-loaded hinge, the robot has to keep the door from closing after opening it. The robot cannot pass through such door using the present controller. A control method for opening such doors will be reported in another paper.

### 5.3   Measurement ability

It is confirmed that the sensor unit was raised 1.5 m above the floor, as Fig. 20 shows, by changing its posture, as Fig. 8 shows. Details of the measurement ability of the arm using the sensor unit are reported in [38].

### 5.4   Mobility

In experiments related to mobility, the robot was controlled using the basic steering method, in which the motion of the head shifts from the head to tail, or using the stair climbing method. The detail of these control methods are reported in [38]. The operator provided the motion of
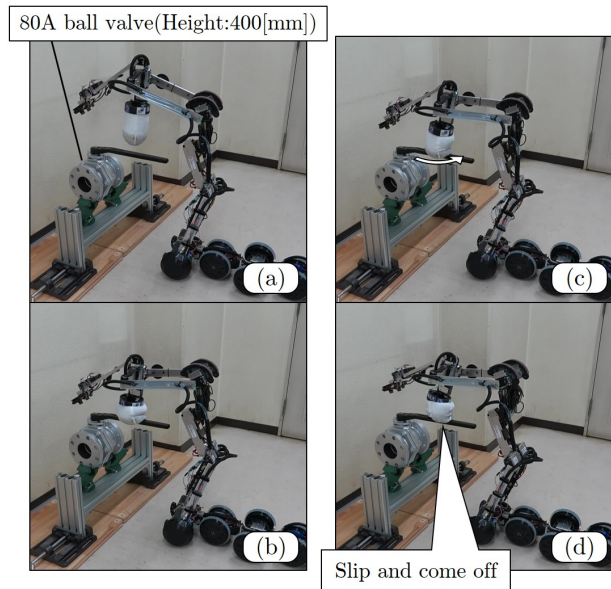
13

Figure 15.   Operating the 80A ball valve. (a) Approaching the valve, (b) grasping the valve, (c) rotating the seventh joint, and (d) slip between the gripper and valve.
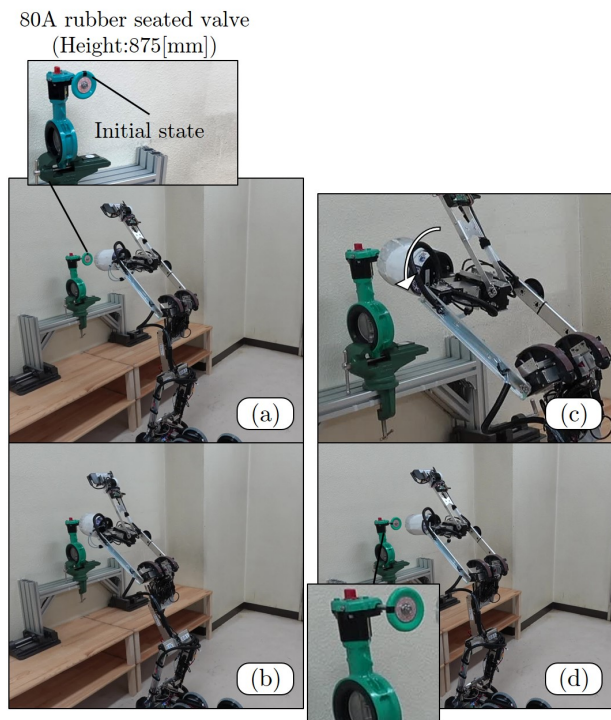


Figure 16.   Operating the 80A rubber seated gate valve. (a) Approaching the valve, (b) grasping the valve, and (c) rotating the valve.

the head using a gamepad while directly looking at the robot without using camera images.

Experiments of the robot with/without the folding arm were carried out using the posture shown in Figs. 9(A)–(E). Table 7 shows the results and Fig. 21 shows the posture of the robot and arm.

When entering the L-shaped path, the width was changed every 50 mm. The minimum width with the arm is 50 mm larger than the robot without the arm because the width of the arm is wider than that of the base part.
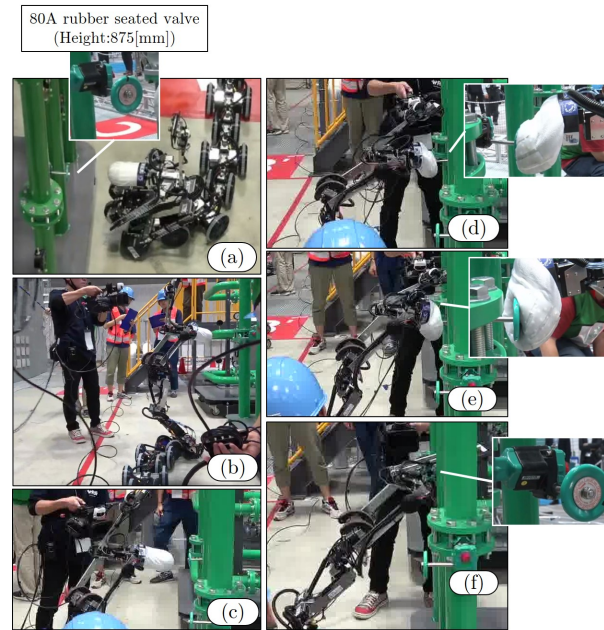
Figure 17. Operating the 80A rubber seated gate valve at WRS2018 [45].

The robot with the arm could climb up the stairs. However, the robot could not climb down the stairs because the arm is heavy and the link of the arm collided with the tread of the stair.

The minimum height of a narrow path depends on the maximum height of the robot. The robot with the arm reduced its maximum height to 220 mm by adopting the posture shown in Fig. 21(C).

The maximum climbable step height in the case with the arm (0.6 m) was smaller than that without the arm (1 m). Main cause of this reduction is the heavy weight of the arm. The arm weight accounts for 40% of the weight of the entire robot. The actuators of the joint of the base part do not have enough torque and mechanical strength to support the weight of the arm, and an overload error or breakage occurred when the robot climbed a step.

Although the robot had the folding arm attached, the maximum width of a trench that the robot could cross did not change. Let the plane in which the robot is first located be the first plane, and the other plane be the second plane. In the case of a 650 mm width trench, the robot without the arm could not reach the second plane because an overload error of the joint occurred. In contrast, the robot with the arm could reach the second plane by using the dummy wheel of the arm, as Fig. 21(E) shows. However, when the tail of the robot left the first plane after the robot moved forward, an overload error of the joint occurred because of the cantilever state of the base part, and the experiment was discontinued. The maximum trench width depends on not the performance of the arm but the performance of the base part.

All design targets related to mobility (Table 2) except for stair descending were accomplished, and the only non-binding target of mobility that was achieved was trench crossing. The failure of the actuator when the robot climbed a step and the misstep while climbing down stairs were caused by the heavy weight of the arm. Hence, reducing the weight of the arm and improving the arm posture are necessary to improve mobility of the robot.

## 6. Conclusion

We developed a folding arm for an articulated mobile robot. The design targets of the arm, that is, its operation, measurement ability, and mobility targets, were set for the task of inspecting an industrial plant, considering the field and missions of WRS2018. The arm has eight joints,
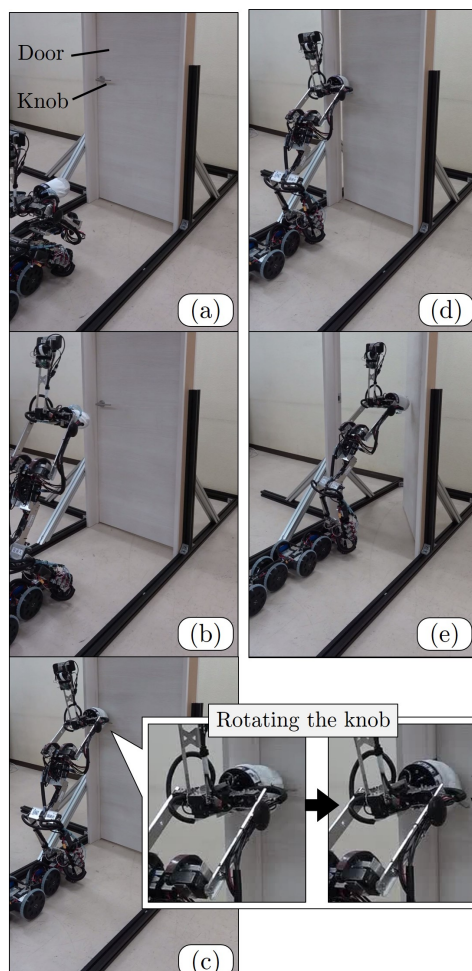
Figure 18.  Opening the door (pushing). (a) Initial state, (b) approaching the door, (c) rotating the knob, and (d) and (e) pushing the door.

Table 7.  Experimental results of mobility.

|  | $T^2$ Snake-4 without the arm | $T^2$ Snake-4 with the arm |
|---|---|---|
| Minimum width of the L-shaped path (mm) | 350 | 400 |
| Stair climbing | Success | Success (climb up) |
| (tread 200 mm, riser 200 mm) |  | Failure (climb down) |
| Minimum height of the narrow path (mm) | 150 | 220 |
| Maximum step height with riser (mm) | 1000 | 600 |
| Maximum trench width (mm) | 600 | 600 |

dummy wheels, a soft gripper, and a sensor unit. The arm can access locations high above the floor and can operate an object. In addition, to reduce the negative effects on the mobility of the robot, the arm can appropriately change its posture using its joints, and can allow dummy wheels to contact the surroundings. The effectiveness of the developed arm was demonstrated by experiments and field tests at WRS2018.

Future tasks are to reduce the weight of the arm and to improve the method of use of the arm when the robot locomotes.
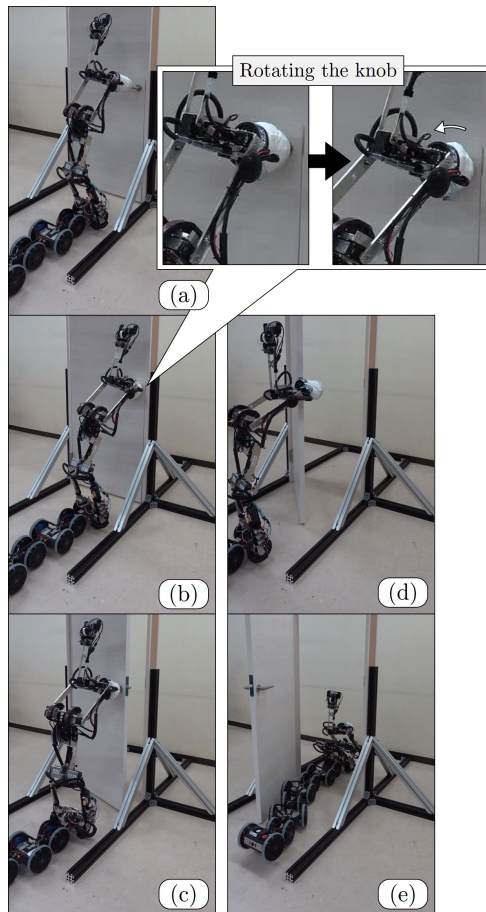
Figure 19.    Opening the door (pulling). (a) Approaching the door, (b) rotating the knob, (c) pulling the door, and (d) and (e) passing through the door.
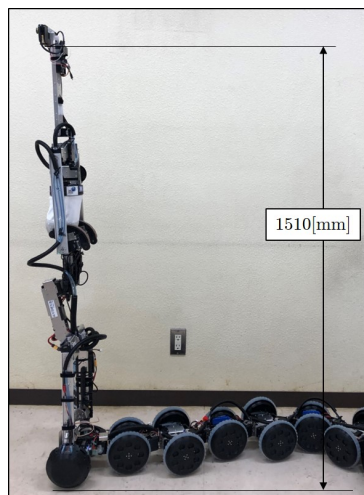


Figure 20.    Test of the posture when the sensor unit reaches its maximum height.
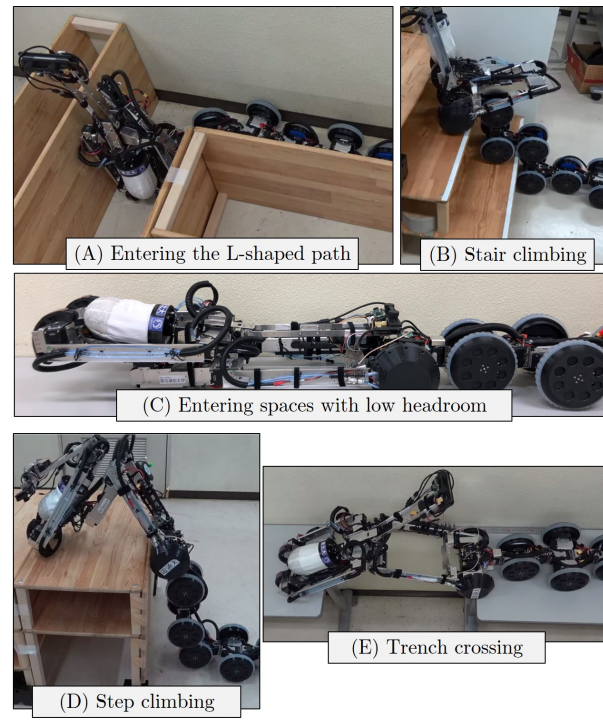
## Acknowledgements

Figure 21. Posture of the robot and arm in mobility tests.

## References

[1] Osuka K, Kitajima H. Development of mobile inspection robot for rescue activities: MOIRA. In: Proc. IEEE/RSJ Int. Conf. on Intelligent Robots and Systems; Las Vegas, Nevada, USA; 2003; p.3373-3377.

[2] Kamegawa T, Yamasaki T, Igarashi H, Matsuno F. Development of the Snake-like Rescue Robot 'KOHGA'. In: Proc. IEEE Int. Conf. on Robotics and Automation; New Orleans, LA, USA; 2004; p.5081-5086.

[3] Borenstein J, Hansen M, Borrell A. The OmniTread OT-4 Serpentine Robot – Design and Performance. J. of Field Robotics; 2007; 24-7:601-621.

[4] Arai M, Tanaka Y, Hirose S, Kuwahara H, Tsukui S. Development of "Souryu-IV" and "Souryu-V:" Serially connected crawler vehicles for in-rubble searching operations. J. of Field Robotics; 2008; 25-1: 31-65.

[5] Ito K, Maruyama H. Semi-autonomous serially connected multi-crawler robot for search and rescue. Advanced Robotics; 2016; 30-7: 489-503.

[6] Scholl KU, Kepplin V, Berns K, Dillmann R. Controlling a Multijoint Robot for Autonomous Sewer Inspection. In: Proc. IEEE Int. Conf. on Robotics and Automation; San Francisco, CA, USA; 2000; p.1701-1706.

[7] Streich H, Adria O. Software Approach for the Autonomous Inspection Robot MAKRO. In: Proc. IEEE Int. Conf. on Robotics and Automation; New Orleans, LA, USA; 2004; p.3411-3416.

[8] Debenest P, Guarnieri M, Hirose S. PipeTron series – Robots for pipe inspection. In: Proc. 3rd Int. Conf. on Applied Robotics for the Power Industry; Foz do Iguassu, Brazil; 2014; p.1-6.

[9] Kakogawa A, Ma S. Design of a multilink-articulated wheeled pipeline inspection robot using only passive elastic joints. Advanced Robotics; 2018; 32-1: 37-50.

[10] Schempf, H, Mutschler E, Gavaert A, Skoptsov G, Crowley W. Visual and nondestructive evaluation inspection of live gas mains using the Explorer[TM]family of pipe robots. J. of Field Robotics; 2010; 27: 217-249.

[11] Rollinson D, Choset H. Pipe Network Locomotion with a Snake Robot. J. of Field Robotics; 2016; 33-3:322-336.

[12] Kamegawa T, Baba T, Gofuku A. V-shift control for snake robot moving the inside of a pipe with helical rolling motion. In: Proc. 2011 IEEE Int. Symp. on Safety, Security and Rescue Robotics;

Kyoto, Japan; 2011; p.1-6.

[13] Fjerdingen AA, Liljebäck P, Transeth AA. A snake-like robot for internal inspection of complex pipe structures (PIKo). In: Proc. IEEE/RSJ Int. Conf. on Intelligent Robots and Systems; St. Louis, USA; 2009; p.5665-5671.

[14] Hirose S, Morishima A. Design and Control of a Mobile Robot with an Articulated Body. The Int. J. of Robotics Research; 1990; 9-2: 99-114.

[15] Hirose S, Morishima A, Tsukagosi S. Design of Practical Snake Vehicle: Articulated Body Mobile Robot KR-II. In: Proc. Fifth Int. Conf. on Advanced Robotics; Pisa, Italy; 1991; p.833-838.

[16] ARGOS Challenge 2018, http://argos-challenge.com/en.

[17] Pellenz J, Jacoff A, Kimura T, Mihankhah E, Sheh R, Suthakorn J. RoboCup Rescue Robot League. In: Bianchi R., Akin H., Ramamoorthy S., Sugiura K. (eds) RoboCup 2014: Robot World Cup XVIII. RoboCup 2014. Lecture Notes in Computer Science, vol 8992. Springer, Cham; 2015. p.673-685

[18] Pratt G, Manzo J. The DARPA Robotics Challenge. IEEE Robotics and Automation Magazine; 2013; 20-2: 10-12.

[19] Fukushima EF, Hirose S, Hayashi T. Basic Manipulation Consideration For The Articulated Body Mobile Robot. In: Proc. IEEE/RSJ Int. Conf. on Intelligent Robots and Systems; Victoria, Canada; 1998; 386-393.

[20] Fukushima EF, Hirose S. Integration of Locomotion and Manipulation Control for Articulated Body Mobile Robots. J. of Robotics Society of Japan; 2000; 18-8: 1112-1121 (in Japanese).

[21] Yamada H, Hirose S. Development of Practical 3-Dimensional Active Cord Mechanism ACM-R4. J. of Robotics and Mechatronics; 2006; 18-3: 305-311.

[22] Yamada H, Takaoka S, Hirose S. A snake-like robot for real-world inspection applications (the design and control of a practical active cord mechanism). Advanced Robotics; 2013; 27-1: 47-60.

[23] Kouno K, Yamada H, Hirose S. Development of Active-Joint Active-Wheel High Traversability Snake-Like Robot ACM-R4.2. J. of Robotics and Mechatronics; 2013; 25-3: 559-566.

[24] Tanaka M, Nakajima M, Suzuki Y, and Tanaka K. Development and Control of Articulated Mobile Robot for Climbing Steep Stairs. IEEE/ASME Trans. on Mechatronics; 2018; 23-2: 531-541.

[25] Tanaka M, Tadakuma K, Nakajima M, Fujita M. Task-Space Control of Articulated Mobile Robots With a Soft Gripper for Operations. IEEE Trans. on Robotics; 2018; 35-1: 135-146.

[26] Yoshida T, Koyanagi E, Tadokoro S, Yoshida K, Nagatani K, Ohno K, Tsubouchi T, Maeyama S, Noda I, Takizawa O, Hada Y. A High Mobility 6-Crawler Mobile Robot Kenaf. In: Proc. 4th Int. Workshop on Synthetic Simulation and Robotics to Mitigate Earthquake Disaster (SRMED2007); Atlanta, USA; 2007; p.38-39.

[27] Nagatani K, Kiribayashi S, Okada Y, Tadokoro S, Nishimura T, Yoshida T, Koyanagi E, Hada Y. Redesign of rescue mobile robot Quince. In: Proc. IEEE Int. Symposium on Safety Security and Rescue Robot; Kyoto, Japan; 2011; p.13-18.

[28] Yamauchi BM. Packbot: a versatile platform for military robotics. In: Proc. Society of Photo-Optical Instrumentation Engineers; Orlando, Florida, USA; 2004; 5422: p.228-237.

[29] Tadakuma K, Takane E, Fujita M, Nomura A, Komatsu H, Konyo M, Tadokoro S. Planar Omnidirectional Crawler Mobile Mechanism-Development of Actual Mechanical Prototype and Basic Experiments. IEEE Robotics and Automation Letters; 2017; 3-1: 395-402.

[30] Chiu Y, Shiroma N, Igarashi H, Sato N, Inami M, Matsuno F. FUMA: Environment Information Gathering Wheeled Rescue Robot with One-DOF Arm. In: Proc. IEEE Int. Workshop on Safety Security and Rescue Robotics; Kobe, Japan; 2005; p.81-86.

[31] Ueda K, Guarnieri M, Hodoshima R, Fukushima EF, Hirose S. Improvement of the remote operability for the arm-equipped tracked vehicle HELIOS IX. In: Proc. IEEE/RSJ Int. Conf. on Intelligent Robots and Systems; Taipei, Taiwan; 2010: p.363-369.

[32] Kamezaki M, Ishii H, Ishida T, Seki M, Ichiryu K, Kobayashi Y, Hashimoto K, Sugano S, Takanishi A, Fujie MG, Hashimoto S, Yamakawa H. Design of Four-Arm Four-Crawler Disaster Response Robot OCTOPUS. In: Proc. IEEE Int. Conf. on Robotics and Automation; Stockholm, Sweden; 2016; p.2840-2845.

[33] Matsumoto N, Tanaka M, Tanaka K, Matsuno F, Tadakuma K. Development of a dispersively storable arm for articulated mobile robot. In: Proc. JSME annual Conference on Robotics and Mechatronics; Kitakyusyu, Japan; 2018; 2P1-J03(in japanese with English summary).

[34] Otsuki K, Watanabe S, Shigetaka S, Kashiwazaki S, Saito T. Wide Range Telescopic Manipulator Mechanism by Aggregated Convex Tapes. In: Proc. JSME Annual Conference on Robotics and Mechatronics; Hamamatsu, Japan; 2012; 2A1-N10 (in japanese with English summary).

[35] Seto N, Canete L, Takahashi T. Development of an atomic interior surveying robot - Prototyping of sampling arm unit using low melting point alloy -. In: Proc. JSME Annual Conference on Robotics and Mechatronics; Kitakyusyu, Japan; 2018; 1P2-M02 (in japanese with English summary).

[36] World Robot Challenge 2018, `http://worldrobotsummit.org/en/wrc2018/`

[37] Tadokoro S, et al., The World robot summit disaster robotics category - achievements of the 2018 preliminary competition. Advanced Robotics; 2019; DOI: 10.1080/01691864.2019.1627244

[38] Tanaka M, Kon K, Nakajima M, Matsumoto N, Fukumura S, Fukui K, Sawabe H, Fujita M, Tadakuma K. Development and Field Test of the Articulated Mobile Robot $T^2$ Snake-4 for Plant Disaster Prevention. Advanced Robotics, accepted.

[39] Fujita M, Tadakuma K, Komatsu H, Takane E, Nomura A, Ichimura T, Konyo M, Tadokoro S. Jamming Layered Membrane Gripper Mechanism for Grasping Differently Shaped-Objects Without Excessive Pushing Force for Search and Rescue. Advanced Robotics; 2018; 32-11: 590-604.

[40] World Robot Challenge 2018, `http://worldrobotsummit.org/en/wrc2018/`

[41] Takase M. Detailed explanation: Robot Kinematics. Ohmsha; 2004. (in Japanese)

[42] Waldron K. Schmiedeler J. Kinematics. In: Siciliano B., Khatib O. (eds) Springer Handbook of Robotics. Springer, Berlin, Heidelberg; 2008; p.11-35.

[43] Plant Disaster Prevention Challenge Day2 (October 18, 2018), `https://youtu.be/ZA8LNPSpeng?t=5255s`

[44] Plant Disaster Prevention Challenge Day4 (October 20, 2018), `https://youtu.be/AzRZnBgJ7ho?t=4737s`

[45] Plant Disaster Prevention Challenge Day3 (October 19, 2018), `https://youtu.be/gdPEIonKuds?t=18958s`